alloys

MDPI

Review

An Overview of High-Entropy Alloys Prepared by Mechanical Alloying Followed by the Characterization of Their Microstructure and Various Properties

Shashanka Rajendrachari

Department of Metallurgical and Materials Engineering, Bartin University, 74100 Bartin, Turkey; shashanka@bartin.edu.tr

Abstract: Some modern alloys, such as high-entropy alloys (HEAs), are emerging with greater acceleration due to their wide range of properties and applications. HEAs can be prepared from many metallurgical operations, but mechanical alloying is considered to be one of the most simple, economical, popular, and suitable methods due to its increased solid solubility, nano-crystalline structure, greater homogeneity, and room-temperature processing. Mechanical alloying followed by the consolidation of HEAs is crucial in determining the various surface and mechanical properties. Generally, spark plasma sintering (SPS) methods are employed to consolidate HEAs due to their significant advantages over other conventional sintering methods. This is one of the best sintering methods to achieve greater improvements in their properties. This review discusses the mechanical alloying of various HEAs followed by consolidation using SPS, and also discusses their various mechanical properties. Additionally, we present a brief idea about research publications in HEA, and the top 10 countries that have published research articles on HEAs. From 2010 to 18 April 2022, more than 7700 Scopus-indexed research articles on all the fields of HEA and 130 research articles on HEA prepared by mechanical alloying alone have been published.

Keywords: microstructure; mechanical alloying; high-entropy alloys; SPS; mechanical properties; ball mill

Citation: Rajendrachari, S. An Overview of High-Entropy Alloys Prepared by Mechanical Alloying Followed by the Characterization of Their Microstructure and Various Properties. *Alloys* **2022**, *1*, 116–132. https://doi.org/10.3390/alloys1020008

Academic Editor: Pavel Krakhmalev

Received: 28 April 2022
Accepted: 29 May 2022
Published: 21 June 2022

1. Introduction

Metals and alloys are very important materials, used significantly for many centuries, starting from hunting in the ancient civilization period to recent advanced electrical applications. We have observed some tremendous improvements in alloys over the past few centuries. Refinement in the crystal structure, composition, microstructure, fabrication methods, and post-treatment are a few of the advances in metallurgy for fabricating various alloys. Alloying of bi-metallic or tri-metallic combinations has been used successfully for many centuries, in which one of the metals is the primary element generally taken in larger concentrations; the secondary metal is used with smaller concentrations [1,2]. However, over the past few decades, extraordinary evolution and progress have been reported on the invention of and improvement in special alloys such as stainless steel, high-speed steels, oxide-dispersed stainless steel, and super-alloys. These alloys comprise simple to complex compositions, depending on the ability of mankind to develop the materials [3]. Generally, they are composed of multi-elements and exhibit high mixing entropy than the entropy of mixing pure metals. As the mixing entropy of the alloy increases, the mixing enthalpy also increases, which allows the addition of more alloying elements. As a result, the properties of the alloy are significantly improved. These types of alloys are called high-entropy alloys [4]. For a few years, researchers have reported more and more complex compositions with high mixing entropies exhibiting tremendous properties. Yeh et al. 2004 [5] and Cantor et al. 2004 [6] reported the possibility of high-entropy alloys using equal proportions of multi-elements. This was a groundbreaking concept and has stimulated research

on developing these types of new materials throughout the world. Since that time, many researchers have published articles in the HEA research field. The trend in the number of publications in the HEA-related field has been increasing every year. Figure 1 shows the number of Scopus-indexed publications related to HEA from 2010 to 18 April 2022.

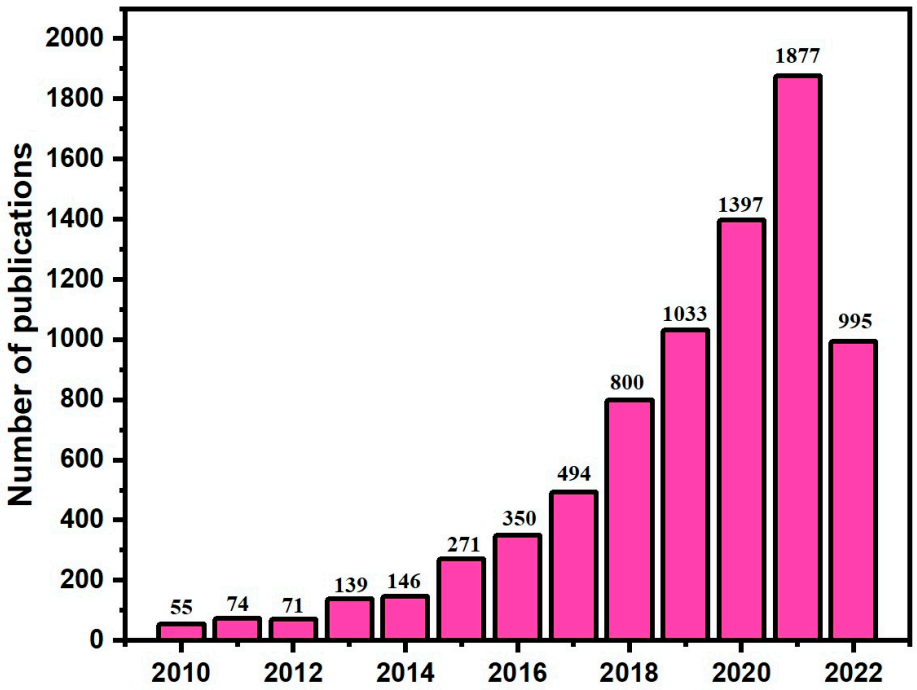

Figure 1. The number of Scopus-indexed publications in the HEA research field from 2010 to 18 April 2022 (data obtained from the Scopus database and plotted by the author).

This shows the popularity of HEA research due to the broad choice of elements to prepare HEAs, their applications, and their unique properties. Figure 2 depicts the ten countries which have published the most research articles on HEAs until 18 April 2022.

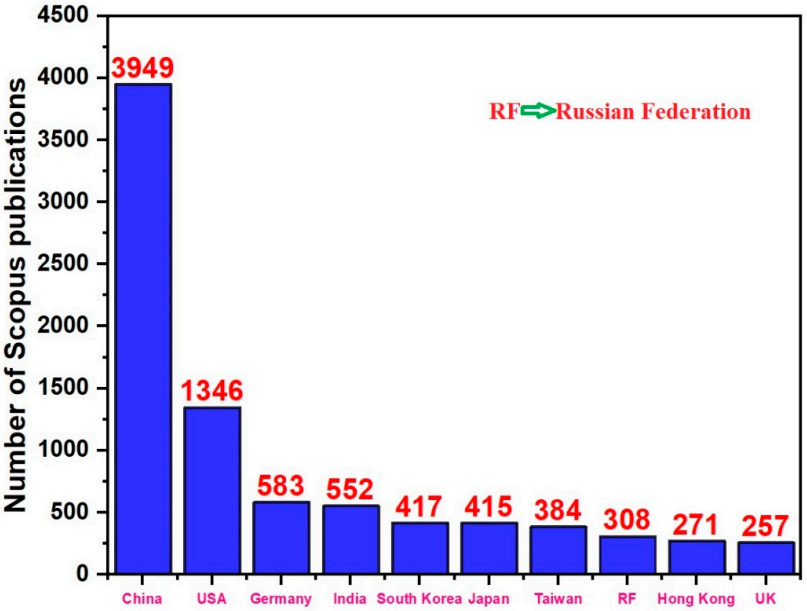

Figure 2. Top 10 countries with the most research articles on HEAs published until 18 April 2022 (data obtained from the Scopus database and plotted by the author).

HEAs are solid solution alloys formed by the combination of multi-metal elements exhibiting simple crystal structures, such as body-centered cubic (BCC), face-centered cubic (FCC), and hexagonal close-packed (HCP) lattices. HEAs can be prepared by adding almost-equal proportions of four or more metals, such as Fe, Cu, Mn, Co, Ti, Cr, Ni, etc. To ensure easy understanding, the normal tri-metallic alloys and multi-elemental high-entropy alloys are presented in Figure 3. Figure 3a shows a normal alloy composed of a combination of three metals, whereas Figure 3b shows an HEA composed of a combination of six different metals.

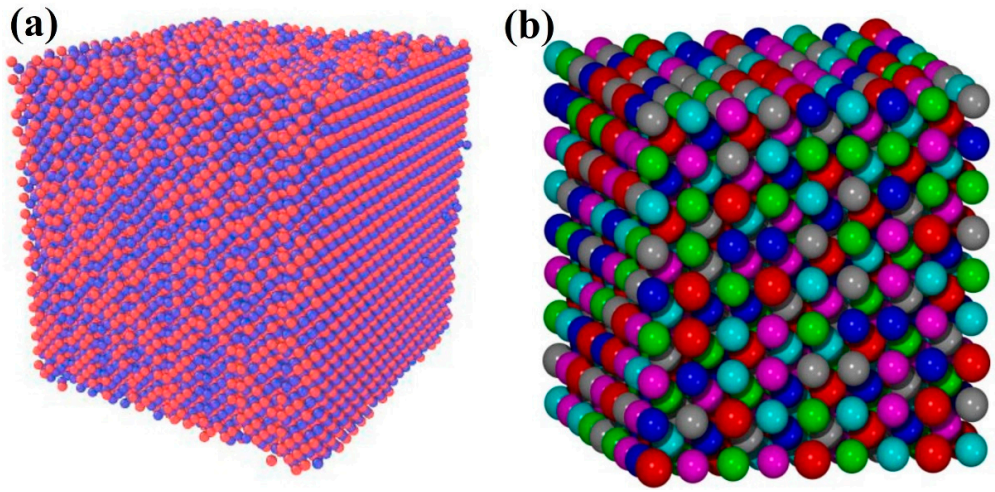

Figure 3. The representation of (**a**) normal bi-metallic alloys and (**b**) multi-elemental high-entropy alloys [7,8].

The properties of any HEAs can be altered according to the required properties by quantitatively and qualitatively changing the composition. HEAs exhibit the unique characteristic of stabilizing a single phase over wide temperature ranges; however, recent studies have revealed that they also exist as multi-phase systems followed by different strengthening mechanisms [9]. Solid solution strengthening and precipitation hardening and their mechanisms, such as twinning and martensitic transformation, play important roles in controlling their mechanical properties. These strengthening mechanisms vary with temperature and strain rate [10]. Generally, conventional alloys such as stainless steel are mechanistically designed using solid solution and precipitation strengthening mechanisms [11]. This results in identifying and controlling the various structural phenomena that dictate the alloys. The same approach is also applicable to HEAs to improve their mechanical properties; as a result, various grades of HEAs can be prepared easily and conveniently. Figure 4 depicts the divinatory stress–strain curve in which micro mechanisms are induced by composition and structural engineering, which generates high-strength alloys.

The use of HEAs has increased extensively in various fields in the past few years, due to their wide range of applications in fields such as medical, chemical, civil, automobile, and aviation. This wide range of applications of HEAs is due to their advantageous properties such as low thermal expansion, good corrosion resistance, high energy absorption, good weldability, and high strength, creep, and wear resistance properties. Modern-day metallurgists have tried to enhance the properties of alloys by mixing or blending almost-equal proportions of multiple elements together, followed by processes such as melting, casting, and forming. However, these methods are not recommended because they need a high-temperature cast; moreover, the formed alloys often become hard and brittle. The main problem conducting research on HEAs lies in the inability to explain the intermetallic compounds and intermediate phases present in quaternary-phase diagrams. These alloy systems contain more than five elements; therefore, it is very difficult to explain their phase diagrams. If any alloy contains two or three elements, it is possible to explain intermetallic compounds and intermediate phases in terms of binary- or ternary-phase

diagrams. However, recent reports have proven that the use of CALPHAD and a database of thermodynamic data could explain phase diagrams, even for HEAs [12,13]. In the late 18th century, a German metallurgist, named Franz Karl Archard, studied multicomponent equal-mass alloys using five to seven elements [7]. He was successful in preparing alloys with altered properties, although the results were not satisfactory. As such, the concept of HEAs was not successfully realized for many years. However, contemporary metallurgists have realized the importance of these alloys and developed new grades of HEAs using arc melting, induction melting [8], sputtering, molecular beam epitaxy [9], thermal spray, laser cladding, electrodeposition [10], and mechanical alloying using a high-energy ball mill [11,12]. Overall, mechanical alloying is proven to be one of the best methods for preparing HEAs, which can reduce the burdens of time, energy, and cost as compared with other conventional metallurgical methods. Therefore, the preparation of HEAs by the ball milling method is famous amongst powder metallurgists, and has been the focus of almost 130 Scopus-indexed research articles published from 2015 to 18 April 2022. This demonstrates the popularity of preparing HEAs through a mechanical alloying method due to the advantages discussed above.

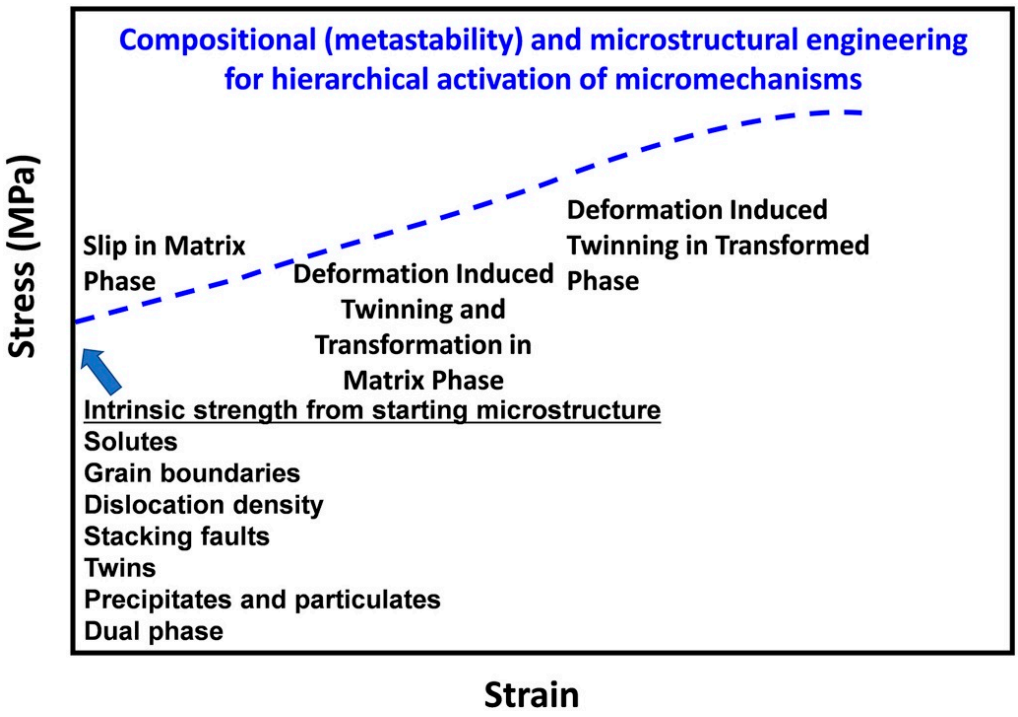

Figure 4. Hypothetical stress–strain curve for a compositionally engineering HEA that transforms and twins during deformation. Adapted with permission from Ref. [10]. Copyright 2021 Elsevier.

To collect the publication data, the author performed a selective search of the Scopus database and tried different combinations of keywords, such as 'high-entropy alloys', and 'mechanical alloying'. Some papers may have been excluded from the Scopus database search due to the use of different keywords, e.g., instead of mechanical alloying, they might have used powder metallurgy or ball milling. This review presents the preparation of various types of HEAs by mechanical alloying followed by their consolidation using SPS. It also focuses on the advantages of using mechanical alloying and SPS methods to process HEAs, as compared with other conventional metallurgical methods followed by studies reported elsewhere. We have attempted to showcase the superiority of mechanical alloying and SPS during the preparation of HEAs.

2. Preparation of HEAs by Mechanical Alloying

Mechanical alloying is a powder metallurgy method generally used to prepare ceramic materials, alloys, and nanomaterials. Generally, mechanical alloying is performed using planetary ball mills [13–17], although sometimes other types of ball mills, such as SPEX mills [18] and shaker rod mills [19], will be used. Milling jars are usually composed of tool steel, stainless steel, and ceramic materials, whereas grinding balls are composed of tungsten carbide, zirconia, chrome steel, stainless steel, alumina, and other ceramic materials [20]. The milling atmosphere may be either dry or wet, based upon the type of materials being milled. Dry milling can be performed in the presence of inert gases, and sometimes nitrogen gases. On the other hand, wet milling can be carried out using toluene [21–23], alcohols, dodecane, cyclohexane, n-heptane, etc. Sometimes, process-controlling agents such as stearic acid are used to reduce the agglomeration. Both wet and dry milling play important roles in controlling the oxidation of materials being milled. The milling speed is also crucial in determining the extent of alloying: increasing the mill speed results in the pinning of grinding balls to the walls of the milling jars, and results in no milling. Therefore, we need to optimize the milling parameters to improve the efficiency of the ball mill. There is plenty of scope to enhance energy efficiency for the bulk production of HEAs by optimizing milling parameters such as the milling time, milling speed, process controlling agents, milling type (dry and wet milling), and ball-to-powder ratio.

Planetary milling involves the mass synthesis of refined objects with perplexed shapes at a low price. It involves the formation of near-net-shaped and homogeneous materials, with less left over as scrap. The fabricated parts can be manufactured with controlled porosity and can be filled by adding other materials with low melting points. Therefore, planetary milling is one of the most widely used plastic deformation methods to achieve the extreme refinement of structure. The advantage of using planetary ball milling to synthesize HEA materials lies in its ability to produce bulk quantities of materials in a solid state, using simple equipment at room temperature. Additionally, planetary-milled powder material reduces the oxidation of the constituent powders due to the short processing time [24,25]. The creation of high-density dislocations, grain boundaries, and the micro-segregation of solute at these defects can lead to an extended solid solution [26]. During milling, the chemical energy is transmitted to crystalline powders and results in deformed random nanocrystalline materials with a longer milling time. Figure 5 shows the experimental ball milling setup.

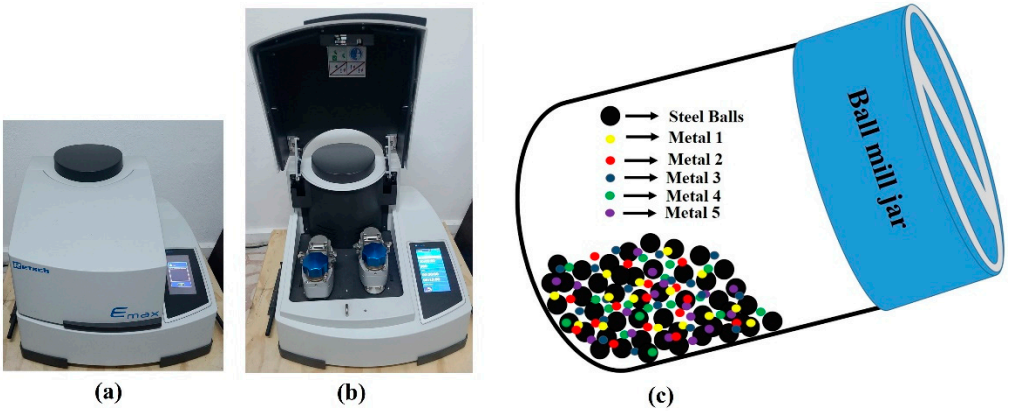

Figure 5. Experimental ball milling set up: (**a**) high-energy planetary ball mill (closed); (**b**) high-energy planetary ball mill (opened view); (**c**) mill jar containing 5 different types of metals (HEA composition) to be alloyed and grinding balls.

Varalakshmi et al. (2008) [27] were the first to prepare AlCrCuFeTiZn HEAs exhibiting a BCC structure with a crystallite size of less than 10 nm using ball milling. Since then, ball milling has become one of the most popular methods for producing HEAs. Varalakshmi et al. reported that the fabricated alloys were even stable above 800 °C during

annealing for 60 min. They claimed to achieve 99% sintered density and a hardness of 2 GPa.

Long et al. fabricated NbMoTaWVTi refractory high-entropy alloys using mechanical alloying followed by SPS [28]. They only obtained BCC-structured HEAs during ball milling for 40 h; however, during consolidation using SPS, a new FCC phase (TiO) precipitated from the BCC matrix out of the HEA.

The precipitation of the new phase is due to oxidation during the processing of HEA. They reported the remarkable mechanical properties due to the formation of a new FCC phase along with the solution and grain boundary strengthening of the BCC matrix of the fabricated HEAs. Finally, they determined the compressive yield strength, fracture strength, and total fracture strain of the SPS-consolidated HEAs as 2709 MPa, 3115 MPa, and 11.4%, respectively [28]. Figure 6 depicts the TEM image and SAED pattern of the mechanically alloyed NbMoTaWVTi HEA powders. From Figure 6, it is confirmed that the precipitated FCC phase is well distributed at the grain boundaries of the BCC matrix. Long et al. also mention that the precipitated FCC phase (TiO) remains in its original crystal structure even at elevated temperatures, due to the increased cooling rate after consolidation.

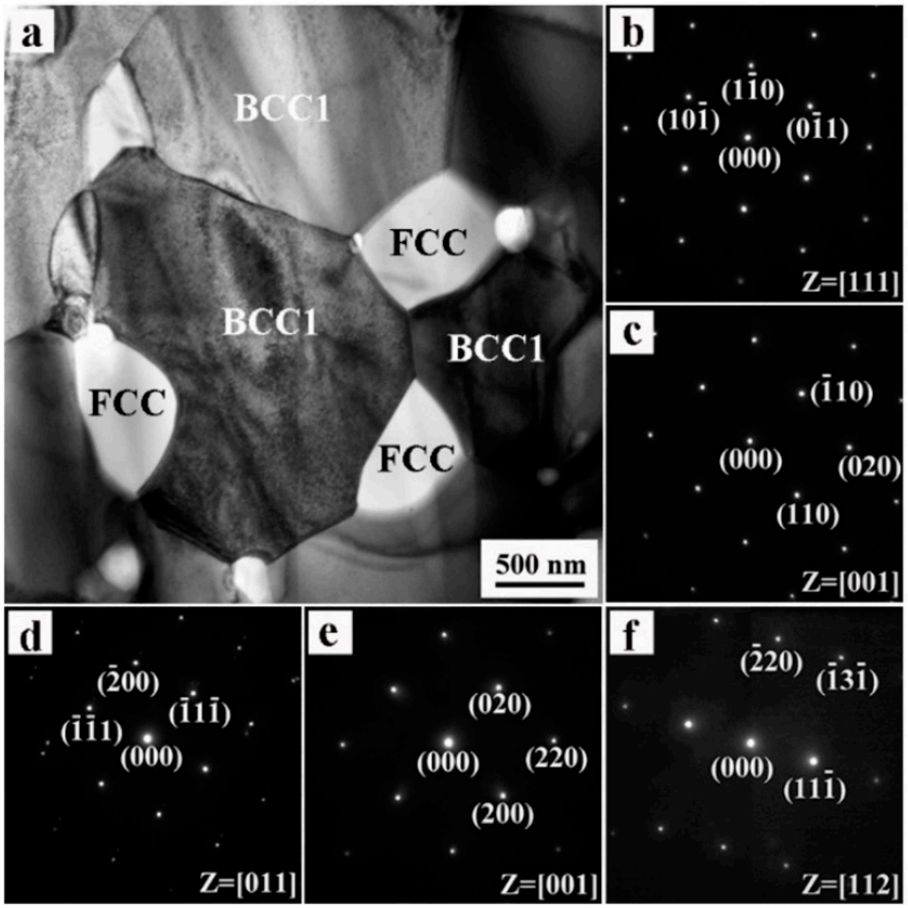

Figure 6. TEM images of the mechanically alloyed NbMoTaWVTi HEA powders: (**a**) bright-field image; (**b**,**c**) SAED patterns of the BCC phase along [29] and [001] zone axes, respectively; (**d**–**f**) SAED patterns of the FCC phase along [011], [001], and [112] zone axes, respectively [28].

Moravcik et al. prepared equiatomic CoCrFeNi HEA using a Pulverisette 6 planetary ball mill for 50 h in the presence of an atmosphere of both argon and nitrogen to study the effect of milling atmosphere and the extent of contamination on bulk HEA [30]. They found that increasing the milling time increases the carbon contamination, and this contamination is due to the dislodging of carbon steel powders from the milling jars and balls. As a result, the SPS-consolidated HEA also showed increased carbon contamination. On the

other hand, the oxygen contamination of HEA also increases with milling time due to the oxidation of fabricated CoCrFeNi alloy during milling. The milling of HEA powders under a nitrogen atmosphere increases nitrogen contamination. Figure 7 depicts the extent of contamination by carbon, oxygen, and nitrogen.

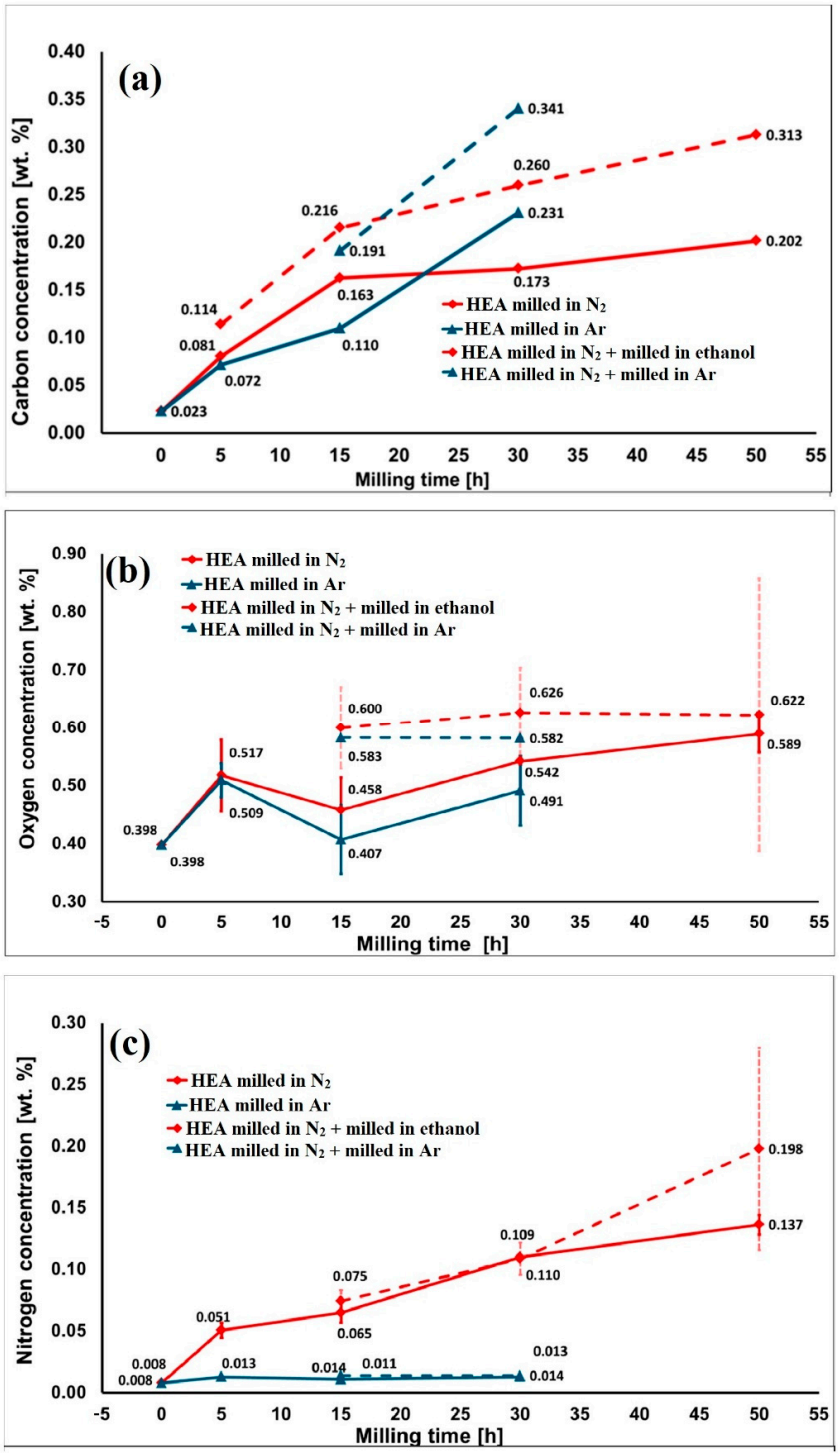

Figure 7. The extent of (**a**) carbon contamination, (**b**) oxygen contamination, and (**c**) nitrogen contamination determined during the milling of HEA alloys in argon and nitrogen atmospheres [30].

Geambazu et al. prepared CoCrFeNiMo0.85 HEAs and studied the corrosion resistance properties of their coating [31]. Mechanical alloying was performed with a Pulverisette 6 planetary ball mill for 30 h, 10:1 ball-to-powder ratio (BPR), mill speed of 350 rpm

under an n-heptane (wet milling) atmosphere using stainless steel balls and jars. The authors successively deposited continuous layers of CoCrFeNiMo0.85 HEAs prepared by mechanical alloying under an argon atmosphere. They compared the microstructures and phases obtained after consolidation by hot pressing and electro-spark deposition (ESD), as shown in Figure 8.

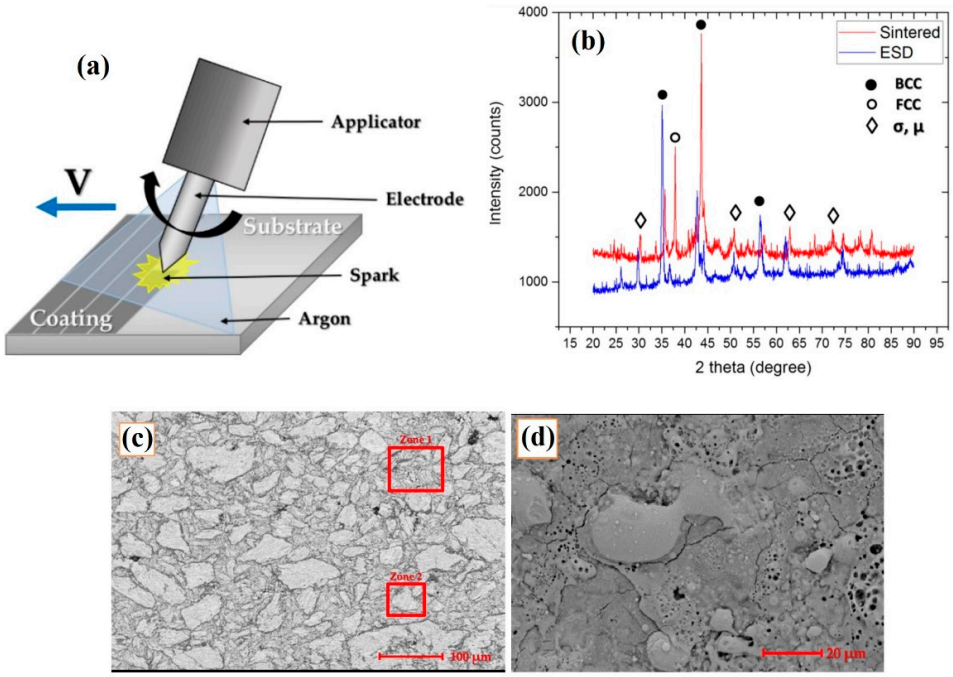

Figure 8. (**a**) Schematic representation of the ESD experimental setup, (**b**) XRD of sintered and ESD-coated HEAs, SEM images of (**c**) sintered and (**d**) ESD-coated HEAs [31].

The XRD results showed increases in μ and σ phases for the ESD-coated HEA, along with FCC and BCC phases. The microstructure of HEAs revealed that the coated HEA exhibited some pores and splats, as shown in the figure [31]. The coated HEA was homogeneous, uniform, and adhesive. Therefore, the pull-off test showed that adhesion was good, with an obtained pull-off resistance of 0.67 MPa. The corrosion resistance of the coating showed a very low corrosion rate of 0.00016 mm/year, indicating the potential use of the fabricated HEA as a corrosion-resistant coating.

Zhu et al. fabricated a TiC-dispersed (10, 20, and 30 wt. %) FeCoNiCuAl HEA by high-energy planetary ball milling for 5 h followed by SPS [32]. XRD and SEM analyses confirmed the uniform distribution of the TiC phase in the FCC and BCC of FeCoNiCuAl HEAs. The microstructures of 0%, 10%, 20%, and 30% TiC-dispersed HEAs (SPS-consolidated) are shown in Figure 9, where the uniform distribution of TiC along with FCC and BCC phases can be observed. Zhu et al. reported that the addition of TiC has increased the hardness from 467 to 768 HV due to the grain and precipitation strengthening. On the other hand, wear resistance of the TiC-dispersed HEA increased up to a certain level; subsequently, it decreased due to the wear mechanism transformation from adhesive to abrasive. They also reported that, at a higher temperature, the wear resistance of prepared HEAs will be significantly reduced due to the oxidative wear mechanism [32].

The CoCrNiCuZn HEAs were prepared by Sun et al. using a planetary ball mill for 60 h with a BPR and mill speed of 20:1 and 300 rpm, respectively [33]. The fabricated HEAs were consolidated by SPS and their microstructures, phases, and mechanical properties were studied. They reported that the fabricated HEA exhibited a crystallite size of 10 nm and a BCC structure after 60 h of milling. After the consolidation of HEA powders by SPS, the authors observed two different FCC phases, as shown in Figure 10, and named them as FCC1 and FCC 2, respectively [33]. They studied the Vickers microhardness and

compressive strength of the SPS-consolidated HEA (900 °C) samples, and the values were found to be 615 HV and 2121 MPa, respectively.

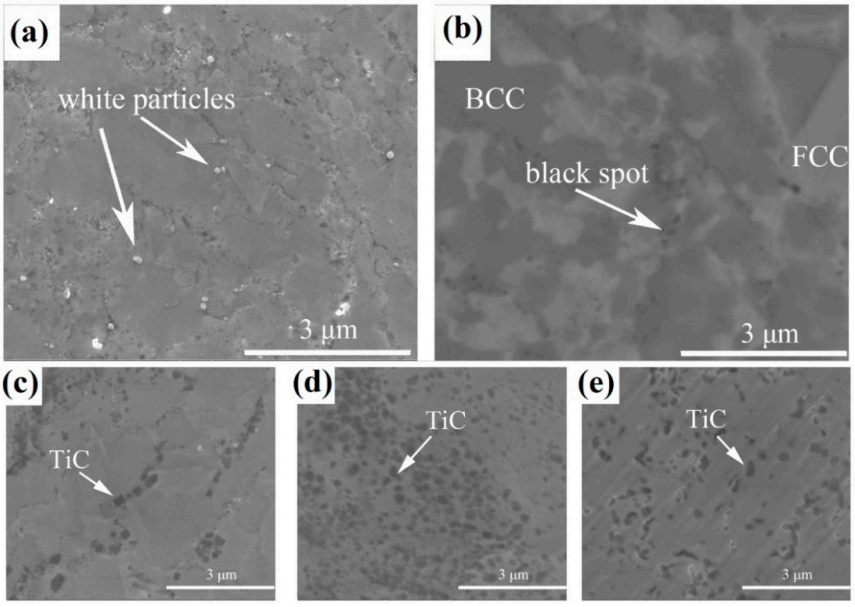

Figure 9. SEM microstructures of (**a**,**b**) 0%, (**c**) 10%, (**d**) 20%, and (**e**) 30% TiC-dispersed HEAs, respectively, consolidated by SPS [32].

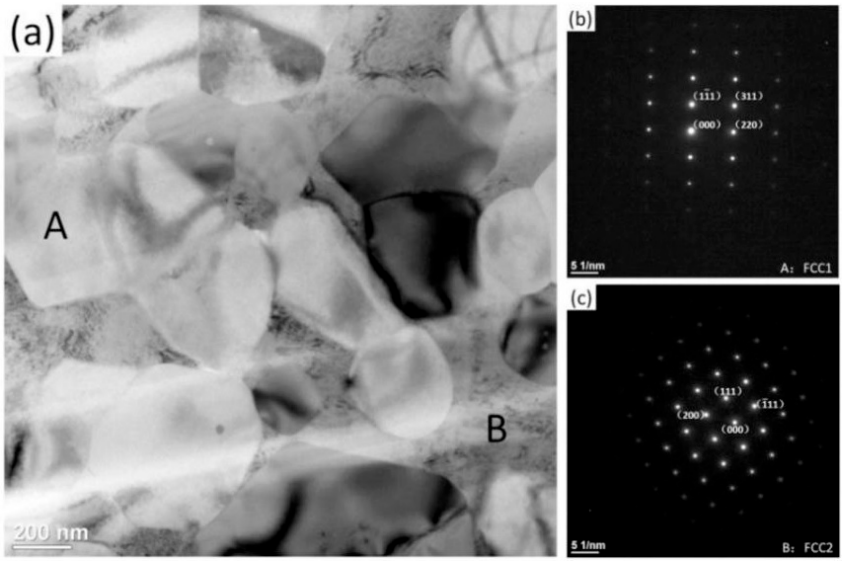

Figure 10. (**a**) TEM image of SPS-consolidated CoCrNiCuZn HEA (900 °C), regions A and B correspond to FCC1 and FCC2 phases, respectively; (**b**,**c**) SEAD pattern of region A and B, respectively [33].

Fourmont et al. (2020) [34] prepared AlCoCrFeNi high-entropy alloys by milling in a planetary ball mill for 28 h after optimizing the milling parameters. They concluded that planetary ball milling is the best method to prepare highly dense HEAs due to the ease of mechanical activation. Therefore, we decided to prepare HEAs by the ball milling method. J. Pan et al. (2018) [35] reported the preparation of Nb25Mo25Ta25W25 and Ti8Nb23Mo23Ta23W23 HEAs by mechanical alloying for 60 h. They reported that the HEA prepared by the ball milling method showed better mechanical properties than four other methods. Tan et al. (2016) [36] synthesized Al2NbTi3V2Zr using a ball mill at 150 rpm and 350 rpm, and reported that only the high-energy mode was more effective in alloying and achieving nano-crystallinity.

The increased use of planetary ball milling to prepare HEAs is due to its various advantages; moreover, one can control the microstructure and properties of HEAs in the mechanical alloying method. After preparing HEAs by mechanical alloying, HEA powders can be consolidated by various conventional and advanced sintering techniques. Among them, SPS is a very advanced and widely used consolidation technique that can offer the highest densification with controlled grain size.

3. Spark Plasma Sintering of Various HEAs

Fabricated HEAs are generally consolidated by different sintering methods, such as hot and cold isostatic pressings, microwave sintering, pressureless sintering, and SPS. Among all, SPS is proven to be one of the more suitable sintering techniques to achieve greater densities and remarkable mechanical properties [37–40]. SPS is an advanced sintering technique that takes only a few minutes to complete; on the other hand, conventional sintering can take hours, or sometimes even days. Due to the internal heating of the sample in SPS, the rate of sintering is higher (up to 300 °C/min); hence, the complete SPS process only takes a few minutes. However, in the case of conventional sintering, heat is provided externally, and as a result, the sintering rate is lower (maximum around 10 °C/min), and it is a slow sintering process. Figure 11 depicts the spark plasma sintering experimental setup.

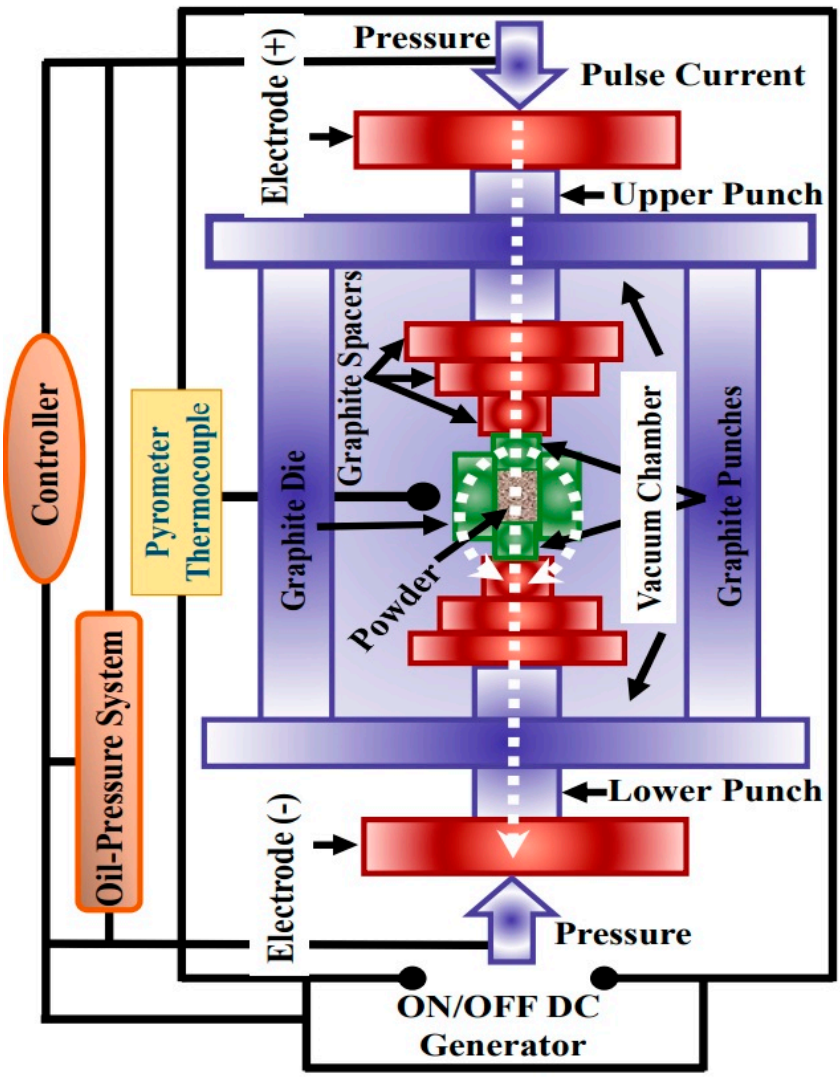

Figure 11. SPS experimental setup [41].

Spark plasma sintering is one of the most effective and advanced sintering techniques among all the sintering methods. It can hinder grain growth during consolidation and also fabricates poorly sinterable materials. It involves the discharging of spark plasma at the gaps of the particles with an on–off electrical current and accelerates the neck formation, as well as the thermal diffusion process of the particles. This restricts the grain growth and results in efficient shrinkage in a shorter time and cleaner grain boundaries for effective interface formation [42]. In the case of SPS, simultaneous applications of temperature and pressure lead to high densification; hence, a dense compact is formed during the sintering process. This results in excellent mechanical properties, such as maximum strength, high hardness, and high density of the materials. All types of materials can be sintered using SPS; the materials which cannot be sintered by conventional sintering can be sintered by the SPS method. SPS is significantly more successful in restricting unwanted sintering reactions due to its high heating rate and shorter holding time.

Nakajo et al. consolidated CoCrFeMnNi HEAs by an SPS technique at temperatures of 973, 1073, and 1173 K, and formed a thin ceramic layer on the top to improve the mechanical properties of the HEA [43]. Surface analysis of the SPS-consolidated HEA layer revealed the presence of a different variety of boride layers, such as M2B-, MB-, and Mn3B4-type borides, which considerably improved their mechanical properties. The surface hardness was 2000–2500 HV due to the formation of a ceramic layer on the HEA surface; elemental analysis revealed that certain elements exhibited characteristic diffusion behaviors. The XRD revealed the formation of only the MB phase at a 1173 K sintering temperature, whereas sintering at 973 K and 1073 K exhibited all three phases—M2B-, MB-, and Mn3B4-type—as shown in Figure 12. The higher temperature of SPS shows the degradation of the M2B and Mn3B4-type, and only the MB ceramic layer will remain. Nakajo et al. concluded that increases in sintering time and temperature do not affect the thickness of the ceramic layer [43].

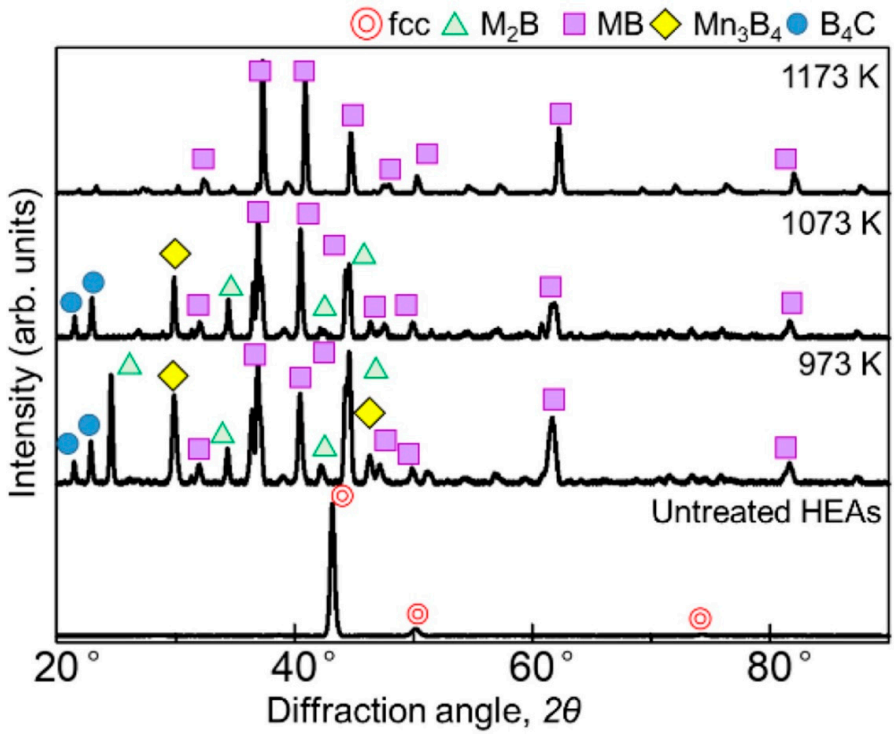

Figure 12. XRD pattern of boronized CoCrFeMnNi HEAs by SPS at 973, 1073, and 1173 K, respectively [43].

Alvi et al. prepared $W_{0.5}(TaTiVCr)_{0.5}$ HEAs followed by consolidation by SPS at 1000, 1200, and 1400 °C sintering temperatures [44]. They studied the phase stability,

compressive strength, and tribology of the consolidated HEAs. The sintered HEA exhibited impressively high compressive strength values of 1136 ± 40 MPa, 830 ± 60 MPa, and 425 ± 15 MPa at 1000, 1200, and 1400 °C, respectively, as shown in Figure 13. They also carried out tribology experiments at 400 °C and found an average friction coefficient and exceptional wear-resistant properties; this was attributed to the formation of solid solution strengthening. Therefore, the authors claimed the possible use of the fabricated HEA, even at a high temperature of 400 °C with a greater degree of stability, high-temperature strength, and excellent wear resistance. These high-temperature properties of fabricated HEAs have enabled their use in plasma-facing materials, rocket nozzles, and industrial tooling [44].

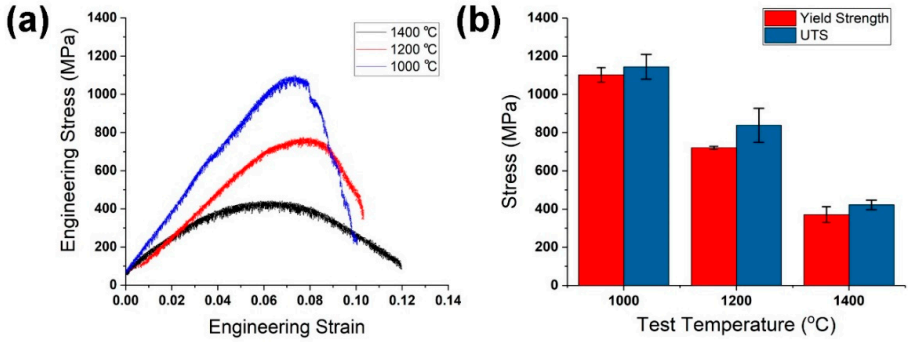

Figure 13. High-temperature (400 °C) (**a**) compressive stress–strain plots and (**b**) yield strength and ultimate tensile strength (UTS) of $W_{0.5}(TaTiVCr)_{0.5}$ HEAs [44].

Kakimoto and Nishimoto fabricated CoCrFeMnNi HEAs through an SPS technique at 1173 K for 10 min under 50 MPa load followed by plasma nitriding to improve their mechanical properties, as shown in Figure 14a [45]. The authors found that plasma nitriding above a temperature of 723 K resulted in the formation of a strong CrN phase, as shown in Figure 14b. The formation of a CrN layer improved the hardness to around 1500 HV, as shown in Figure 14c, with excellent wear and pitting corrosion-resistant properties.

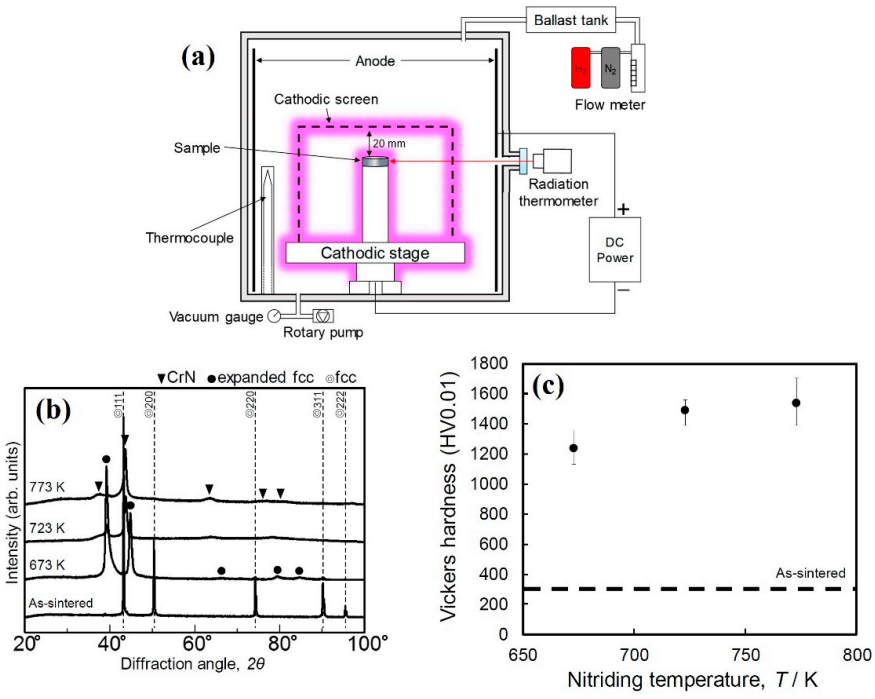

Figure 14. (**a**) Experimental setup of plasma nitriding, (**b**) XRD, and (**c**) Vickers microhardness of plasma-nitrided SPS-consolidated CoCrFeMnNi samples at 673, 723, and 773 K, respectively [45].

Rymer et al. produced ultra-fine-grain-structured CrFeCoNi HEAs through the SPS technique at 1050 °C temperature under 50 MPa uniaxial pressure for 13 min [46]. The microstructure of the sintered HEA confirmed the formation of ultra-fine grains, as shown in Figure 15. The mechanical properties such as the microhardness and tensile strength of SPS-consolidated CrFeCoNi HEA were excellent, and their properties were further improved by the combination of SPS and equal-channel angular pressing, as reported by the authors [46].

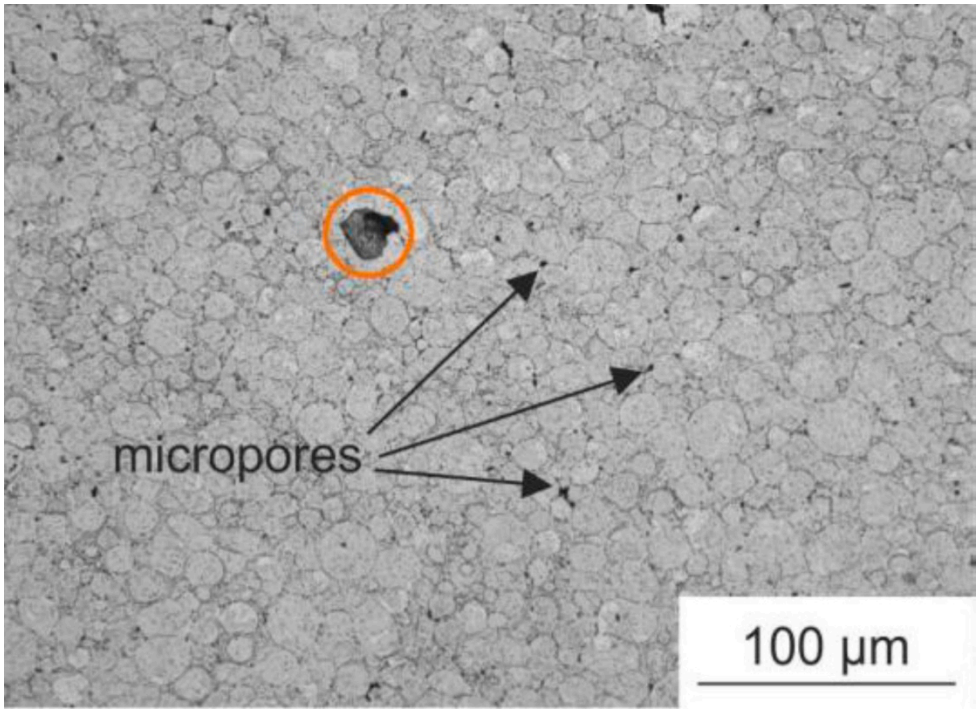

Figure 15. Microstructure of SPS-consolidated CrFeCoNi HEA exhibiting ultra-fine grains [46].

Shkodich et al. fabricated refractory HfTaTiNbZr HEAs by SPS at 1300 °C for 10 min [47]. They found that the combined effect of mechanical alloying and SPS could significantly improve the mechanical properties as compared with SPS-consolidated samples without mechanical alloying. The combined effect increased the Vickers hardness to 10.7 GPa and density to ≈99%; on the other hand, the SPS-consolidated samples without mechanical alloying only showed Vickers microhardness values of 5.8 to 6.4 GPa. Therefore, Shkodich et al. concluded the importance of combining the effect of mechanical alloying and SPS.

Murali et al. (2018) [48] consolidated mechanically alloyed AlCoCrCuFeTix HEA powders using the SPS method at a temperature of 1173 K and a pressure of 45 MPa. The grain size of the consolidated HEA was found to be 45–50 nm. Joo et al. (2017) [49] reported that the average grain size of the CoCrFeMnNi HEA increased slightly, from 11 nm to 280 nm, after consolidation by SPS at 1173 K. Wang et al. (2016) [50] consolidated CoCr2-xCuFeNix HEAs using SPS; they reported a slight increase in the grain size from ten nanometers to several hundred nanometers before and after SPS, respectively. Thus, the grain growth during SPS is relatively reduced, and it is possible to retain the nanostructure even after sintering. Table 1 depicts the mechanical alloying and SPS of various HEAs fabricated by various researchers.

Table 1. The mechanical alloying and SPS of various HEAs fabricated by various researchers.

Composition of HEA	Type of Ball Mill Used	Ball Milling Parameters	SPS Parameters	Mechanical Properties	References
CoCrFeNiMnAl	Planetary ball mill	60 h, 15:1 BPR, argon atmosphere, 200 rpm mill speed, stearic acid as PCA	20 mm diameter, 800 °C for 10 min under 50 MPa axial pressure in an argon atmosphere	Vickers hardnessof 662 HV and compressive strength of 2142 MPa	[51]
AlCrCuFeZn	High-energy planetary ball mill P-5	50 h, 15:1 BPR, argon atmosphere, 250 rpm mill speed, n-heptane as PCA	800 °C for 5 min under 50 MPa uniaxial pressure in an argon atmosphere	91% density and 627 HV microhardness	[52]
CrMoNbWV	Planetary mill P-4	5 h, 20:1 BPR, argon atmosphere, 350/700 rpm mill speed	Graphite die of 40 mm, 1200, 1300, and 1400 °C under 50 MPa uniaxial pressure for 5 min	Compressive strength of 2700–2870 MPa and microhardness of 1266 HV	[53]
AlCoCrFe	P-5 high-energy ball mill	15 h, 10:1 BPR, 300 rpm mill speed, toluene as PCA	1000 °C under 30 MPa uniaxial pressure for 3 min	Microhardness of 1050 HV	[54]
FeCoCrNiAl	Planetary Ball Mill PM 100	35 h, 10:1 BPR, 250 rpm mill speed	20 mm diameter, 1000 °C for 5 min under 60 MPa axial pressure	Elastic modulus of 260 GPa and microhardness of 550 HV	[55]
CoCrFeNiMoNb	Fritsch P5 high-energy ball mill	30 h, 10:1 BPR, toluene as PCA	20 mm diameter, 900 and 1000 °C for 5 min under 30–50 MPa axial pressure	Microhardness of 710 HV and relative density of 94% was achieved	[56]
$AlCoCrFeNiTi_{0.5}$	High-energy ball mill	24 h, 10:1 BPR, argon atmosphere, 250 rpm mill speed	20 mm diameter, 1100 °C for 8 min under 60 MPa axial pressure	Microhardness of 762 HV, elastic modulus of 160 GPa	[57]
CoCrFeMnNi	Fritsch P5 high-energy ball mill	15 h, 10:1 BPR, 300 rpm mill speed, toluene as PCA	15 mm diameter, 1173 K for 5 min under 60 MPa axial pressure	96% relative density was achieved	[29]

4. Conclusions

This review has discussed the research on HEAs and their fabrication by mechanical alloying followed by SPS. It has also covered why mechanical alloying is a popular and suitable method for preparing HEAs. In other conventional methods, such as melting and casting, the phase transitions will generally take place during cooling; this depends on the mobility and distribution of constituent elements present in the alloys. Sometimes, the cooling rate and atomic arrangement can affect the diffusivity of the elements present in HEA, which can influence the microstructure of the alloy. HEAs prepared from these methods exhibit dendritic microstructures with interdendritic segregations, which results in the formation of a more dominant single phase by reducing the possibility of precipitation of secondary phases. The mechanical alloying process produces heat during milling, and the produced heat is sufficient to induce phase formation. Various milling parameters also affect the phase transformation by severe plastic deformation followed by increases in lattice strain and dislocation density. On the other hand, phase transformations may also be affected by lattice distortion and slow diffusivity during SPS. As detailed in the Discussion, mechanical alloying may cause contamination, oxidation, and agglomeration during the

milling of HEAs, but can be strongly minimized by optimizing the milling parameters. As discussed in this article, PM alloys with improved properties and microstructures mainly rely on the composition of the alloy and the manufacturing methods. Designing alloys plays an important role in controlling the morphology, microstructure, and phase transformation. One such consolidation method is SPS, which has many advantages over other conventional sintering methods. We have discussed how SPS affects the microstructure, mechanical properties, and density of HEAs. We have showcased the number of Scopus-indexed publications on HEAs and the fabrication of HEAs, particularly by mechanical alloying, up to 18 April 2022. We have also listed the top 10 countries which have published the most Scopus-indexed articles in the HEA research field. Trends in the number of publications on HEAs are increasing every year due to the challenges, scope, lacunae, unique properties, and applications of HEAs.

Funding: The author gratefully acknowledges the Bartin University Scientific Research Projects Unit, Turkey, for providing financial support to conduct the research (project number: 2021-FEN-A-007).

Institutional Review Board Statement: Not applicable.

Informed Consent Statement: Not applicable.

Data Availability Statement: Not applicable.

Conflicts of Interest: The author declares no conflict of interest.

References

1. Ding, J.; Xu, H.; Li, X.; Liu, M.; Zhang, T. The similarity of elements in multi-principle element alloys based on a new criterion for phase constitution. *Mater. Des.* **2021**, *207*, 109849. [CrossRef]
2. Joseph, J.; Senadeera, M.; Chao, Q.; Rana, S.; Gupta, S. Computational design of thermally stable and precipitation-hardened Al-Co-Cr-Fe-Ni-Ti high entropy alloys. *J. Alloys Compd.* **2021**, *888*, 161496. [CrossRef]
3. Yeh, J.W. *Overview of High-Entropy Alloys, High-Entropy Alloys, Fundamentals and Applications*; Gao, M.C., Yeh, J.W., Liaw, P.K., Zhang, Y., Eds.; Springer: Cham, Switzerland, 2016.
4. Wu, Y.; Liaw, P.K.; Zhang, Y. Preparation of Bulk TiZrNbMoV and NbTiAlTaV High-Entropy Alloys by Powder Sintering. *Metals* **2021**, *11*, 1748. [CrossRef]
5. Yeh, J.W.; Chen, S.K.; Lin, S.J.; Gan, J.Y.; Chin, T.S.; Shun, T.T.; Tsau, C.H.; Chang, S.Y. Nanostructured high-entropy alloys with multiple principal elements: Novel alloy design concepts and outcomes. *Adv. Eng. Mater.* **2004**, *6*, 299–303. [CrossRef]
6. Cantor, B.; Chang, I.T.H.; Knight, P.; Vincent, A.J.B. Microstructural development in equiatomic multicomponent alloys. *Mater. Sci. Eng. A* **2004**, *375–377*, 213–218. [CrossRef]
7. Cui, Z.; Zhou, X.; Meng, Q. Atomic-Scale Mechanism Investigation of Mass Transfer in Laser Fabrication Process of Ti-Al Alloy via Molecular Dynamics Simulation. *Metals* **2020**, *10*, 1660. [CrossRef]
8. Wang, S. Atomic Structure Modeling of Multi-Principal-Element Alloys by the Principle of Maximum Entropy. *Entropy* **2013**, *15*, 5536–5548. [CrossRef]
9. Rivera-Díaz-del-Castilloa, P.E.J.; Fu, H. Strengthening mechanisms in high-entropy alloys: Perspectives for alloy design. *J. Mater. Res.* **2018**, *33*, 2970–2982. [CrossRef]
10. Mishra, R.S.; Haridas, R.S.; Agrawal, P. High entropy alloys—Tunability of deformation mechanisms through integration of compositional and microstructural domains. *Mater. Sci. Eng. A* **2021**, *812*, 141085. [CrossRef]
11. Joele, M.; Matizamhuka, W.R. A Review on the High Temperature Strengthening Mechanisms of High Entropy Superalloys (HESA). *Materials* **2021**, *14*, 5835. [CrossRef]
12. Moravcikova-Gouvea, L.; Moravcik, I.; Pouchly, V.; Kovacova, Z.; Kitzmantel, M.; Neubauer, E.; Dlouhy, I. Tailoring a Refractory High Entropy Alloy by Powder Metallurgy Process Optimization. *Materials* **2021**, *14*, 5796. [CrossRef] [PubMed]
13. Moravcikova-Gouveaa, L.; Moravcika, I.; Omastab, M.; Veselýc, J.; Cizeka, J.; Minárikc, P.; Cupera, J.; Záděrab, A.; Jana, V.; Dlouhy, I. High-strength Al0.2Co1.5CrFeNi1.5Ti high-entropy alloy produced by powder metallurgy and casting: A comparison of microstructures, mechanical and tribological properties. *Mat. Charact.* **2020**, *159*, 110046. [CrossRef]
14. Smith, C.S. *Four Outstanding Researchers in Metallurgical History*; American Society for Testing and Materials: Baltimore, MD, USA, 1963.
15. Zhang, Y.; Zuo, T.T.; Zhi, T.; Gao, M.C.; Dahmen, K.A.; Liaw, P.K.; Lu, Z.P. Microstructures and properties of high-entropy alloys. *Prog. Mater. Sci.* **2014**, *61*, 1–93. [CrossRef]
16. Zou, Y.; Ma, H.; Spolenak, R. Ultrastrong ductile and stable high-entropy alloys at small scales. *Nat. Commun.* **2015**, *6*, 7748. [CrossRef]
17. Yao, C.Z.; Zhang, P.; Liu, M.; Li, G.R.; Ye, J.Q.; Liu, P.; Tong, Y.X. Electrochemical preparation and magnetic study of Bi–Fe–Co–Ni–Mn high-entropy alloy. *Electrochim. Acta* **2008**, *53*, 8359–8365. [CrossRef]

18. Youssef, K.M.; Zaddach, A.J.; Niu, C.; Irving, D.L.; Koch, C.C. A Novel Low-Density, High-Hardness, High-entropy Alloy with Close-packed Single-phase Nanocrystalline Structures. *Mater. Res. Lett.* **2014**, *3*, 95–99. [CrossRef]
19. Wei, J.; Weimin, W.; Hao, W.; Jinyong, Z.; Yucheng, W.; Fan, Z.; Zhengyi, F. Alloying behavior and novel properties of CoCrFeNiMn high-entropy alloy fabricated by mechanical alloying and spark plasma sintering. *Intermetallics* **2015**, *56*, 24–27.
20. Nayak, A.K.; Shashanka, R.; Chaira, D. Effect of Nanosize Yittria and Tungsten Addition to Duplex Stainless Steel During High Energy Planetary Milling. *IOP Conf. Ser. Mater. Sci. Eng.* **2016**, *115*, 012008. [CrossRef]
21. Gómez-Esparza, C.D.; Baldenebro-López, F.; González Rodelas, L.; Baldenebro-López, J.; Martínez-Sánchez, R. Series of nanocrystalline NiCoAlFe(Cr, Cu, Mo, Ti) highentropy alloys produced by mechanical alloying. *Mater. Res.* **2016**, *19*, 39. [CrossRef]
22. Sun, C.; Li, P.; Xi, S.; Zhou, Y.; Li, S.; Yang, X. A new type of high entropy alloy composite Fe18Ni23Co25Cr21Mo8WNb3C2 prepared by mechanical alloying and hot pressing sintering. *Mater. Sci. Eng. A.* **2018**, *728*, 144. [CrossRef]
23. Vaidya, M.; Muralikrishna, G.M.; Murty, B.S. High-entropy alloys by mechanical alloying: A review. *J. Mater. Res.* **2019**, *34*, 664–686. [CrossRef]
24. Shashanka, R. Effect of Sintering Temperature on the Pitting Corrosion of Ball Milled Duplex Stainless Steel by using Linear Sweep Voltammetry. *Anal. Bioanal. Electrochem.* **2018**, *10*, 349–361.
25. Shashanka, R.; Uzun, O.; Chaira, D. Synthesis of nano-structured duplex and ferritic stainless steel powders by dry milling and its comparison with wet milling. *Arch. Metall. Mater.* **2020**, *65*, 5–14.
26. Shashanka, R.; Chaira, D. Phase transformation and microstructure study of nano-structured austenitic and ferritic stainless steel powders prepared by planetary milling. *Powder. Technol.* **2014**, *259*, 125–136.
27. Varalakshmi, S.; Kamaraj, M.; Murty, B.S. Synthesis and characterization of nanocrystalline AlFeTiCrZnCu high entropy solid solution by mechanical alloying. *J. Alloys Compd.* **2008**, *460*, 253–257. [CrossRef]
28. Long, Y.; Su, K.; Zhang, J.; Liang, X.; Peng, H.; Li, X. Enhanced Strength of a Mechanical Alloyed NbMoTaWVTi Refractory High Entropy Alloy. *Materials* **2018**, *11*, 669. [CrossRef]
29. Vaidya, M.; Karati, A.; Marshal, A.; Pradeep, K.G.; Murty, B.S. Phase evolution and stability of nanocrystalline CoCrFeNi and CoCrFeMnNi high entropy alloys. *J. Alloys Compd.* **2019**, *770*, 1004. [CrossRef]
30. Moravcik, I.; Kubicek, A.; Moravcikova-Gouvea, L.; Adam, O.; Kana, V.; Pouchly, V.; Zadera, A.; Dlouhy, I. The Origins of High-Entropy Alloy Contamination Induced by Mechanical Alloying and Sintering. *Metals* **2020**, *10*, 1186. [CrossRef]
31. Geambazu, L.E.; Cotrut, C.M.; Miculescu, F.; Csaki, I. Mechanically Alloyed CoCrFeNiMo0.85 High-Entropy Alloy for Corrosion Resistance Coatings. *Materials* **2021**, *14*, 3802. [CrossRef]
32. Zhu, T.; Wu, H.; Zhou, R.; Zhang, N.; Yin, Y.; Liang, L.; Liu, Y.; Li, J.; Shan, Q.; Li, Q.; et al. Microstructures and Tribological Properties of TiC Reinforced FeCoNiCuAl High-Entropy Alloy at Normal and Elevated Temperature. *Metals* **2020**, *10*, 387. [CrossRef]
33. Sun, Y.; Ke, B.; Li, Y.; Yang, K.; Yang, M.; Ji, W.; Fu, Z. Phases, Microstructures and Mechanical Properties of CoCrNiCuZn High-Entropy Alloy Prepared by Mechanical Alloying and Spark Plasma Sintering. *Entropy* **2019**, *21*, 122. [CrossRef] [PubMed]
34. Fourmont, A.; Gallet, S.L.; Politano, O.; Desgranges, C.; Baras, F. Effects of planetary ball milling on AlCoCrFeNi high entropy alloys prepared by Spark Plasma Sintering: Experiments and molecular dynamics study. *J. Alloys Compd.* **2020**, *820*, 153448. [CrossRef]
35. Pan, J.; Dai, T.; Lu, T.; Ni, X.; Dai, J.; Li, M. Microstructure and mechanical properties of Nb25Mo25Ta25W25 and Ti8Nb23Mo23Ta23W23 high entropy alloys prepared by mechanical alloying and spark plasma sintering. *Mater. Sci. Eng. A* **2018**, *738*, 362–366. [CrossRef]
36. Tan, X.R.; Zhang, G.P.; Zhi, Q.; Liu, Z.X. Effects of milling on the microstructure and hardness of Al2NbTi3V2Zr high entropy alloy. *Mater. Des.* **2016**, *109*, 27–36. [CrossRef]
37. Shashanka, R.; Chaira, D.; Chakravarty, D. Fabrication of Nano-Yttria Dispersed Duplex and Ferritic Stainless Steels by Planetary Milling Followed by Spark Plasma Sintering and Non-Lubricated Sliding Wear Behaviour Study. *J. Mater. Sci. Eng. B* **2016**, *6*, 111–125.
38. Shashanka, R.; Chaira, D.; Kumara Swamy, B.E. Effect of Y_2O_3 nanoparticles on corrosion study of spark plasma sintered duplex and ferritic stainless steel samples by linear sweep voltammetric method. *Arch. Metall. Mater.* **2018**, *63*, 749–763.
39. Shashanka, R. Non-lubricated dry sliding wear behavior of spark plasma sintered nano-structured stainless steel. *J. Mater. Environ. Sci.* **2019**, *10*, 767–777.
40. Rayappa, S.M.; Shamanth, V.; Sharath, P.C.; Shashanka, R.; Hemanth, K. A Review on Spark Plasma Sintering of Duplex Stainless Steels. *Mater. Today Proc.* **2021**, *45*, 138–144.
41. Nisar, A.; Zhang, C.; Boesl, B.; Agarwal, A. Unconventional Materials Processing Using Spark Plasma Sintering. *Ceramics* **2021**, *4*, 20–39. [CrossRef]
42. Kopeliovich, D. Spark Plasma Sintering. SubsTech Substances & Technologies. Available online: http://www.substech.com/dokuwiki/doku.php?id=spark_plasma_sintering (accessed on 20 March 2022).
43. Nakajo, H.; Nishimoto, A. Boronizing of CoCrFeMnNi High-Entropy Alloys Using Spark Plasma Sintering. *J. Manuf. Mater. Process.* **2022**, *6*, 29. [CrossRef]
44. Alvi, S.; Waseem, O.A.; Akhtar, F. High Temperature Performance of Spark Plasma Sintered $W0.5(TaTiVCr)_{0.5}$ Alloy. *Metals* **2020**, *10*, 1512. [CrossRef]

45. Karimoto, T.; Nishimoto, A. Plasma-Nitriding Properties of CoCrFeMnNi High-Entropy Alloys Produced by Spark Plasma Sintering. *Metals* **2020**, *10*, 761. [CrossRef]
46. Rymer, L.M.; Lindner, T.; Frint, P.; Löbel, M.; Lampke, T. Designing (Ultra)Fine-Grained High-Entropy Alloys by Spark Plasma Sintering and Equal-Channel Angular Pressing. *Crystals* **2020**, *10*, 1157. [CrossRef]
47. Shkodich, N.; Sedegov, A.; Kuskov, K.; Busurin, S.; Scheck, Y.; Vadchenko, S.; Moskovskikh, D. Refractory High-Entropy HfTaTiNbZr-Based Alloys by Combined Use of Ball Milling and Spark Plasma Sintering: Effect of Milling Intensity. *Metals* **2020**, *10*, 1268. [CrossRef]
48. Murali, M.; Kumaresh, B.S.P.; Majhi, J.; Vallimanalan, A.; Mahendran, R. Processing and characterisation of nano crystalline AlCoCrCuFeTix high-entropy alloy. *Powder. Metall.* **2018**, *61*, 139–148. [CrossRef]
49. Joo, S.H.; Kato, H.; Jang, M.J.; Moon, J.; Kim, E.B.; Hong, S.J.; Kim, H.S. Structure and properties of ultrafine-grained CoCrFeMnNi high-entropy alloys produced by mechanical alloying and spark plasma sintering. *J. Alloys Compd.* **2017**, *698*, 591–604. [CrossRef]
50. Wang, P.; Cai, H.; Cheng, X. Effect of Ni/Cr ratio on phase, microstructure and mechanical properties of NixCoCuFeCr2-x (x=1.0, 1.2, 1.5, 1.8 mol) high entropy alloys. *J. Alloys Compd.* **2016**, *662*, 20–31. [CrossRef]
51. Wang, C.; Ji, W.; Fu, Z. Mechanical alloying and spark plasma sintering of CoCrFeNiMnAl high-entropy alloy. *Adv. Powder Technol.* **2014**, *25*, 1334–1338. [CrossRef]
52. Cardoso, K.R.; Bruno da Silva, I.; Leonardo de Souza, V.; Bepe, A.M. Mechanical alloying and spark plasma sintering of AlCrCuFeZn high entropy alloy. *Mater. Sci. Technol.* **2020**, *36*, 1861–1869. [CrossRef]
53. Razumov, N.; Makhmutov, T.; Kim, A.; Shemyakinsky, B.; Shakhmatov, A.; Popovich, V.; Popovich, A. Refractory CrMoNbWV High-Entropy Alloy Manufactured by Mechanical Alloying and Spark Plasma Sintering: Evolution of Microstructure and Properties. *Materials* **2021**, *14*, 621. [CrossRef]
54. Praveen, S.; Anupam, A.; Tilak, R.; Kottada, R.S. Phase evolution and thermal stability of AlCoCrFe high entropy alloy with carbon as unsolicited addition from milling media. *Mater. Chem. Phys.* **2018**, *210*, 57. [CrossRef]
55. Colombini, E.; Rosa, R.; Trombi, L.; Zadra, M.; Casagrande, A.; Veronesi, P. High entropy alloys obtained by field assisted powder metallurgy route: SPS and microwave heating. *Mater. Chem. Phys.* **2018**, *210*, 78. [CrossRef]
56. Praveen, S.; Murty, B.S.; Kottada, R.S. Effect of molybdenum and niobium on the phase formation and hardness of nanocrystalline CoCrFeNi high entropy alloys. *J. Nanosci. Nanotechnol.* **2014**, *14*, 8106. [CrossRef] [PubMed]
57. Moravcik, I.; Cizek, J.; Gavendova, P.; Sheikh, S.; Guo, S.; Dlouhy, I. Effect of heat treatment on microstructure and mechanical properties of spark plasma sintered AlCoCrFeNiTi0.5 high entropy alloy. *Mater. Lett.* **2016**, *174*, 53. [CrossRef]